

Analytical and Numerical Flash-Algorithms for Track Fits

M. Dima

*Dept. of Physics, Campus Box 390
University of Colorado,
Boulder, CO-80309*

Flash-algorithm track-reconstruction routines with speed factors 3000-4000 in excess those of traditional iterative routines are presented. The methods were successfully tested in the alignment of the Test Beam setup for the ATLAS Pixel Detector MCM-D modules, yielding a 60 fold increase in alignment resolution over iterative routines, for the same amount of allocated CPU time.

I. INTRODUCTION

In many particle physics experiments high-precision alignment can be performed provided there is sufficient data and enough computer (CPU) time allocated. While statistics may suffice for many experiments, CPU time can only be decreased through the use of flash reconstruction routines. For instance in pixel detectors, alignment parameters can be tuned iteratively to satisfy good track reconstruction in all events. However, reconstruction of all tracks in all events, for each iteration in alignment parameter space¹, is CPU exhausting and in practice can only be applied to blocks of tracks. If the track fits themselves are also iterative [2], double-nesting of iteration loops occurs and CPU times reach on the order of months. On the other hand if track fits are semi/analytical, CPU times drop 3-4 orders in magnitude and such an approach becomes feasible.

The paper starts with the basic χ^2 fit, examines the validity of the standard quadratic approximation for χ^2 and presents analytical and semi-analytical track reconstruction algorithms, together with CPU-clocked examples². The methods were developed gradually from the simple case of straight tracks (magnetic field free environment, or high momentum tracks), to the more demanding case of helical tracks. The Test Beam setup of the ATLAS Pixel Detector [3] MCM-D modules [4] was used as prototype example for the applied methods, although the latter methods are general and applicable to a number of detectors using tracks.

¹An example of an analytical alignment procedure (*vs.* an iterative one) is illustrated in [1] for the SLD End-Cap Čerenkov Ring Imaging Detector.

²The tests were performed on a DEC-ALPHA 878 machine, with EV 5.6 processor at 433 MHz, 640 MB RAM, and running under OSF1 V4.0. Coding was performed in FORTRAN.

II. GENERAL FITS

The general expression for χ^2 in a fit is the sum of normalised residuals over the set of experimental points:

$$\chi^2 \stackrel{\text{def}}{=} \sum_{j=1}^N \Delta_j^2 / \sigma_{j(\Delta)}^2 \quad (1)$$

where the error of the j^{th} -residual $\sigma_{j(\Delta)}$ is related to the direction $|\Delta_j\rangle$ into which this residual is pointing:

$$\sigma_{j(\Delta)}^2 = \frac{\langle \Delta_j | \sigma_j^2 | \Delta_j \rangle}{\langle \Delta_j | \Delta_j \rangle} \quad (2)$$

$\langle A | B \rangle$ denoting scalar product. This leads to:

$$\chi_{\text{exact}}^2 = \sum_{j=1}^N \frac{\langle \Delta_j | \Delta_j \rangle^2}{\langle \Delta_j | \sigma_j^2 | \Delta_j \rangle} \quad (3)$$

More often however, a quadratic³ approximation of χ_{exact}^2 is used:

$$\chi_{\text{approx}}^2 \stackrel{\text{def}}{=} \sum_{j=1}^N \langle \Delta_j | \sigma_j^{-2} | \Delta_j \rangle \quad (4)$$

with the equivalent residual error:

$$\sigma_{j(\Delta)}^2 = \frac{\langle \Delta_j | \Delta_j \rangle}{\langle \Delta_j | \sigma_j^{-2} | \Delta_j \rangle} \quad (5)$$

If a track impacts a point's error ellipsoid at $n = \text{tg}(\theta_{\text{incid}})$ with respect to one of the principal axes, then approximating $|\Delta_j\rangle$ as perpendicular to the trajectory, the two σ 's can be written as:

$$\begin{aligned} \sigma_{\text{exact}}^2 &\simeq \frac{\sigma_{xy}^2 + n^2 \sigma_z^2}{1 + n^2} \\ \sigma_{\text{approx}}^2 &\simeq \frac{1 + n^2}{\sigma_{xy}^{-2} + n^2 \sigma_z^{-2}} \end{aligned} \quad (6)$$

both reducing to σ_{xy}^2 or σ_z^2 for tracks impacting along one of the principal axes.

³ $\langle \Delta_j | \sigma_j^{-2} | \Delta_j \rangle = \Delta_x^2 / \sigma_x^2 + \Delta_y^2 / \sigma_y^2 + \Delta_z^2 / \sigma_z^2$, for σ_j assumed diagonal.

For the prototype considered, the Test Beam stand for the ATLAS Pixel MCM-D modules, the tracking elements were 4 Sirocco strip Detectors, the setup allowing 1 or 2 Pixel Detectors/Modules to be under evaluation. The Sirocco strips were mounted along $\Delta z = 1.4$ m of beam-line with a tolerance of ± 0.5 mm. The strips, 30 μm wide, provided a resolution of 4 μm in the x- and y-directions, while the Pixels, 50 $\mu\text{m} \times 400\mu\text{m}$, a resolution on the order of 14 $\mu\text{m} \times 180\mu\text{m}$ depending on the cast technology [4] of the chips. The error matrices of the Test Beam stand Telescope points had thus associated ellipsoids with aspect ratios of 1:125, the difference between fitting a 3D-line to these σ 's and one to spherical σ 's being 0.1 μm in the Telescope's mid-plane.

The difference between χ^2_{exact} and χ^2_{approx} depends strongly on the impact angle of the track onto the individual error ellipsoids:

$$\frac{\Delta\chi^2}{\chi^2_{exact}} = \frac{(\sigma_{xy}/\sigma_z)^2 + (\sigma_z/\sigma_{xy})^2 - 2}{(n + 1/n)^2} \quad (7)$$

For the Telescope setup the track's impact angle was on the average 0.15 mrad, with a corresponding $\Delta\chi^2/\chi^2_{exact}$ on the order of 0.02%. When the tracks impact however at an arbitrary angle, $\Delta\chi^2/\chi^2_{exact}$ can reach as high as 3000 for the current σ_z/σ_{xy} ratio, even if $\Delta\sigma^2/\sigma_{exact}^2$ is on the order of unity.

For tracks impacting all points at a constant angle ("stiff"-tracks), $\Delta\chi^2$ is constant along the trajectory and the two methods yield identical results. If the track is measured however piecewise in two different sub-systems, or it is composed of an ensemble of points with different σ 's (different types of detectors), then even for straight tracks the two solutions differ. For tracks bending in magnetic field, the track's impact angle changes continuously along the track, $\Delta\chi^2$ following as:

$$d\left(\frac{\Delta\chi^2}{\chi^2_{exact}}\right) / \frac{\Delta\chi^2}{\chi^2_{exact}} = \frac{dn}{n} \cdot \frac{1 - n^2}{1 + n^2} \quad (8)$$

Within the 1.4 m of the Telescope, the 180 GeV/c tracks used bend in the $B = 1.4$ T magnetic field equivalently to $\Delta\chi^2/\chi^2_{exact} \simeq 0.02\%$ up front and 16% downstream, the approximative method pulling the fit increasingly tighter towards the end - on the order of 0.5 μm per point. The effect is evidently insignificant, both in the Telescope setup, as well as in the real B-physics context of ATLAS ($p \geq 1$ GeV/c, $B = 2.0$ T, $\Delta z \simeq 0.14$ m, or a point to point change of less than 4 % per %- $\Delta\chi^2$).

III. LINE FITS

In most cases it is possible to interchange the non-linear expression (3) with its quadratic approximation (4), allowing analytical solutions to be given for "stiff-tracks" *i.e.* - particle out of magnetic field, weak field

with respect to track momentum, or distance travelled small with respect to existing resolution.

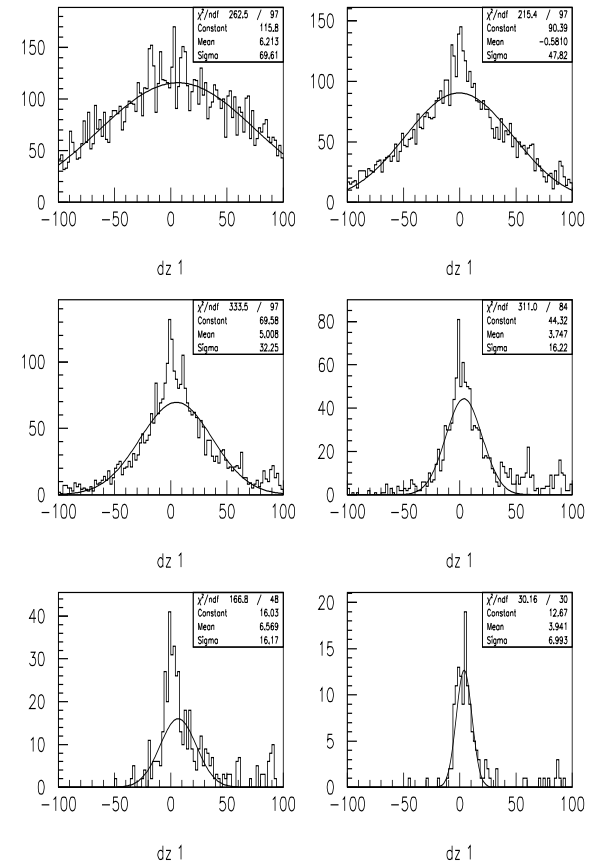


FIG. 1. Translational alignment parameter (Δz) histograms for blocks of 2, 4, 8, 20, 40 and 80 tracks. The effective number of track-fits in each histogram is $\simeq 3$ million. Although in the Telescope setup the alignment lever arm for Δz is very low (0.15 $\mu\text{m}/\text{mm}$, with a $\sigma = 4 \mu\text{m}$ detector resolution), the plots show a dramatic improvement in Δz resolution with increasing N_{block} , the electronics noise being cut-down by a factor of $1/\sqrt{N_{block}}$. The approach demands however extensive CPU power, analytical solutions being needed in order to keep the problem within the capabilities of existing resources. All figures are in mm.

The simplest fit is for $\sigma_j^2 = \sigma^2 \cdot \mathbf{1} = \text{const.}$:

$$\chi^2 = \sum_{j=1}^N \vec{\Delta}_j^2 = \text{min.} \quad (9)$$

Parametrising the tracks as:

$$\vec{r} = \vec{r}_0 + \lambda \vec{n} \quad (10)$$

with $\vec{n}^2 = 1$ and $\vec{r}_0 \cdot \vec{n} = 0$, equation (9) becomes:

$$\chi^2 = \sum_{j=1}^N \vec{\delta}_j^2 = \text{min.} \quad (11)$$

where $\vec{\delta}_j = \vec{r}_j - \vec{r}_0 - \lambda_j \vec{n}$. The minimum condition implies locally $\lambda_j = \vec{r}_j \cdot \vec{n}$ and globally:

$$\begin{aligned}\vec{r}_0 &= (\mathbf{1} - \vec{n}\vec{n}) \langle \vec{r} \rangle \\ \mathbf{M} \vec{n} &= \mu_0 \vec{n}\end{aligned}\quad (12)$$

where $\langle \vec{r} \rangle$ denotes average over measured points, and $\mathbf{M} = \langle \vec{r} \vec{r} \rangle - \langle \vec{r} \rangle \langle \vec{r} \rangle$ spread ellipsoid of points around $\langle \vec{r} \rangle$. The 3 eigen-values of \mathbf{M} represent the length of the track (μ_0), and the two transversal variances to the line-fit.

For $\sigma_j^2 = \text{diag}(\sigma_x^2, \sigma_y^2, \sigma_z^2) = \text{const.}$ equation (11) holds again, however in normalised form, with $\vec{r}_i \rightarrow \sigma^{-1} \vec{r}_i$, $\vec{r}_0 \rightarrow \sigma^{-1} \vec{r}_0$ and $\vec{n} \rightarrow \sigma^{-1} \vec{n}$. Adapted to the geometry of the Telescope this solution has been clocked to $0.033 \mu\text{s}/2\text{D-fit}$ and $2.6 \mu\text{s}/3\text{D-fit}$ vs. $6100 \mu\text{s}/3\text{D-fit}$ for a MINUIT [5] driven routine. CPU-wise this permits the use of up to 2000 tracks per alignment block, giving a $\sqrt{N_{block}}$ increase in alignment resolution, all at a CPU cost proportional to N_{block} . In the Test Beam setup the tracks impact the Sirocco planes at almost normal incidence, the “lever arm” for Δz misalignments being on the order of $0.15 \mu\text{m}/\text{mm}$. With the existing Sirocco resolution ($\simeq 4 \mu\text{m}$) the resolving power for Δz is on the order of 27 mm. This can be improved substantially by increasing the number of tracks in the inner loop of the alignment parameter tuning, the effect being illustrated in figure 1.

Holding allocated CPU time constant, the increase in speed can be equivalenced to alignment resolution increase by increasing the statistics in the inner loop. In the case of the Telescope setup the resolution increase is 60 fold, any multi-tile pixel detector benefiting from this high precision alignment method⁴.

An improvement to the example considered would be to include in the track fit also the Pixel Demonstrator points. This would mean fitting to points with different error ellipsoids and the impossibility of “absorbing” all σ ’s into \vec{r}_0 and \vec{n} in an unique way, as done previously. For such $\sigma_i^2 \neq \sigma_j^2$ cases, the solution is given by a set of self-consistent equations:

$$\begin{aligned}\lambda_j &= \frac{\vec{n} \cdot \sigma_j^{-2} (\vec{r}_j - \vec{r}_0)}{\vec{n} \cdot \sigma_j^{-2} \vec{n}} \\ \vec{r}_0 &= \langle \vec{r} \rangle - \langle \lambda \rangle \vec{n}\end{aligned}$$

⁴Respectively from higher purities and efficiencies in the physics program. For example B-events can be selected with very high performance by applying a minimally missing \vec{p}_\perp correction to the m_π evaluated vertex mass [6,7]. In the ATLAS context \vec{p}_\perp would most likely be referenced to the axis of the jet containing the B sub-jet. The method depends crucially on vertexing accuracy, for instance at SLD [7] yielding B-events with sample purities on the order of 91-99 % and 65-20% corresponding efficiencies.

$$\vec{n} = \frac{\langle \lambda \vec{r} \rangle - \langle \lambda \rangle \langle \vec{r} \rangle}{\langle \lambda^2 \rangle - \langle \lambda \rangle^2} \quad (13)$$

solvable semi-analytically in approximately 3 iterations, starting from the previous analitically exact solution.

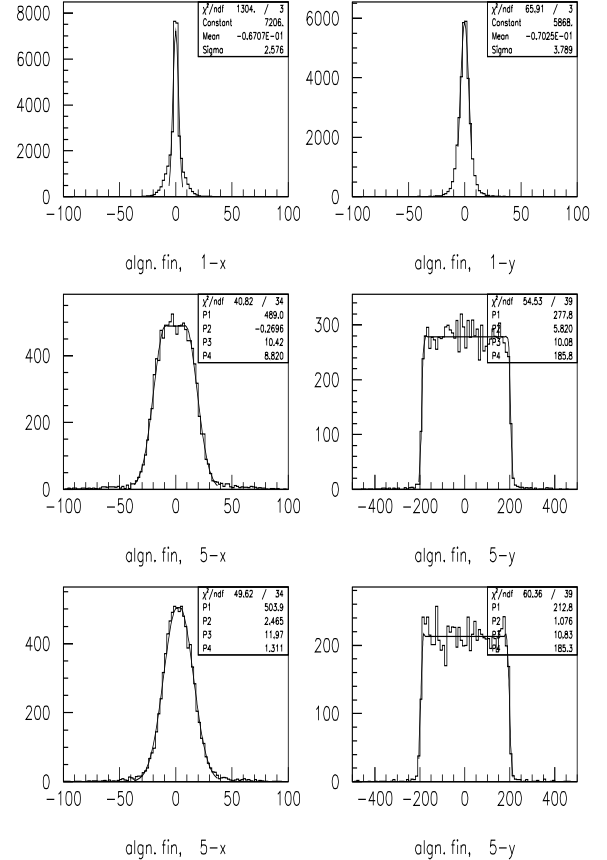


FIG. 2. Final alignment residuals for the Telescope’s Sirocco plane-1 (top), $\sigma_x \simeq 3 \mu\text{m}$, $\sigma_y \simeq 4 \mu\text{m}$, and for two Pixel Detectors under test, cast in different technologies (middle and bottom). The equal *side*-resolution of the Pixels (fit parameter P3, $\sigma_{\text{side}} \simeq 11 \mu\text{m}$) in the *x* and *y*-directions gives confidence that the alignment conducts to physically meaningful results. Fit parameter P4 gives the single-hit resolution of the pixel “hat” ($\sigma_{\text{hat}} = 1 \dots 10 \mu\text{m}$). The center “thinning” of the Sirocco *x*-residuals (from a gaussian) by $\simeq 1 \mu\text{m}$ was due to the residual magnetic field of the Spectrometer Magnet, as Lorentz drift of the charge carriers in the strips. All figures are in μm .

The approach used in this paper was to tune the alignment by looping over the reconstruction of 2000 tracks, the alignment residuals of the Telescope Sirocco plane-1 being shown in figure 2 (top). The Pixel Detectors under evaluation were to first order aligned analitically (exact solution), and subsequently tuned in a fashion similar to that of the Sirocco planes, in order to compensate for the effect of the low *y*-resolution on the better *x*-resolution. The difference between the Pixel demonstrator measured and Telescope predicted positions of the

track hits is shown in figure 2 (middle and bottom) for a set of two Pixel Detectors under test. The identical *side*-resolution of the pixels in the x and y -directions (fit parameter P3) - expected from uniform technology on the chip - gives credit that the alignment conducted to physically tangible results.

IV. HELIX FITS

Track fits over small arcs of helices are very sensitive to the fluctuations of the experimental points. The radius of curvature (giving the momentum, or conversely the magnetic field) has consequently a large error, due to the points moving within their error bars. To reduce the errors of such “weak” parameters, fits to collections of tracks - experiencing the same conditions (magnetic field in this case) are used. Iterative fit routines consum however between 90000-300000 μs /3D helix-fit, the previously illustrated method (figure 1) being inapplicable in this case. On the other hand, although desired, flash semi-analytical algorithms for helix-fits are non-trivial to derive. Most of contemporary High Energy Physics experiments however involve large energies and the helical tracks span typically less than 1° of an arc (0.2° in the case of the Telescope). It is possible then in such cases to perform 3D-helix fits semi-analytically, by perturbatively curving a line-fit into a helix-fit. The helix equations are:

$$\begin{aligned} d_t \vec{p} &= \frac{ec^2}{E} \vec{p} \times \vec{B} \\ d_t \vec{r} &= c^2 \vec{p} / E \end{aligned} \quad (14)$$

where E is the particle’s energy, \vec{p} its momentum and \vec{B} the magnetic field. The solution to equations (14) is:

$$\vec{r} = \vec{r}_0 + \lambda \vec{n} + \frac{\lambda^2}{2!} f\left(\frac{\lambda}{R}\right) \mathbf{F} \vec{n} + \frac{\lambda^3}{3!} g\left(\frac{\lambda}{R}\right) \mathbf{G} \vec{n} \quad (15)$$

where $\lambda = \vec{v}_0 t = \omega R t$ is a “linear” distance travelled by the particle, $\vec{\omega} = |e|c^2 \vec{B}/E$ the helical rotation pulsation, $\vec{n} = \vec{p}_0/p_0$ the direction of engagement of the particle onto the magnetic field, $\vec{n}_B = e\vec{B}/|e|B$, $R = p_0/|e|B$ a parameter related to the radius of curvature of the helix $R_{\text{helix}} = R\sqrt{1 - (\vec{n} \cdot \vec{n}_B)^2}$, $f(\zeta)$ and $g(\zeta)$ two functions:

$$\begin{aligned} f(\zeta) &= \frac{2!}{\zeta^2} (1 - \cos \zeta) \stackrel{\zeta \rightarrow 0}{\simeq} 1 \\ g(\zeta) &= \frac{3!}{\zeta^3} (\zeta - \sin \zeta) \stackrel{\zeta \rightarrow 0}{\simeq} 1 \end{aligned} \quad (16)$$

respectively \mathbf{F} and \mathbf{G} two tensors:

$$\begin{aligned} \mathbf{F} &= \times \vec{C} \\ \mathbf{G} &= \vec{C} \vec{C} - \vec{C}^2 \cdot \mathbf{1} \end{aligned} \quad (17)$$

that satisfy $\mathbf{F}^\dagger = -\mathbf{F}$, $\mathbf{G}^\dagger = \mathbf{G}$, $\mathbf{F}\mathbf{G} = \mathbf{G}\mathbf{F} = \vec{C}^2\mathbf{F}$, $\mathbf{F}^2 = \mathbf{G}$, and $\mathbf{G}^2 = -\vec{C}^2\mathbf{G}$. The vector \vec{C} is \vec{n}_B/R .

It is evident that for $R \rightarrow \infty$ (or equivalently $\lambda \rightarrow 0$), expression (15) reduces to the parametrisation of the line (10) used in performing line fits - which is the requirement for the perturbative approach. In most experiments the third order approximation $f(\zeta) \simeq 1$ and $g(\zeta) \simeq 1$ holds up to the following limiting factors:

- **geometric** - the arc of helix should not exceed a length beyond the approximation validity for $f(\zeta)$ and $g(\zeta)$. This is related to the demanded resolution σ and the particle’s momentum:

$$p \geq \frac{\lambda}{16(\sigma/\lambda)^{1/3}} \simeq 5 \text{ GeV/c} \quad (18)$$

where in the above, λ and σ are expressed in [m] and p in [GeV/c]. The value for the momentum is for the Telescope setup.

- **dE/dx** - the loss of energy along the trajectory determines a “tighter” helix, the deviation:

$$\sigma = \frac{\lambda^2 E}{2\pi p^2 c^2} \left(\frac{dE}{dx} \right) \quad (19)$$

needing to be smaller than 4 times the allowed tolerance in the Pixel plane.

- **multiple scattering** - multiple deviations from the direction of flight add up to a displacement of:

$$\sigma \simeq 0.6\lambda\theta_{rms} \quad (20)$$

where λ is expressed in [mm], θ_{rms} [8] in [mrad] and σ in [μm]. This should determine an error in the Pixel plane no larger than the allowed tolerance.

The semi-analytical helix fit procedure has 3 steps:

1. Estimation of \vec{n} , the engagement direction of the particle onto the magnetic field. This is obtained with small CPU demand via a 3D line flash-fit to the first 3-4 points of the trajectory. The vector \vec{n} is an eigen-vector of $\mathbf{M} = \langle \vec{r} \vec{r} \rangle - \langle \vec{r} \rangle \langle \vec{r} \rangle$, hence any perturbation $\delta\mathbf{M} = \mathbf{M}_{\text{helix}} - \mathbf{M}_{\text{line}}$ changes it only to second order, and for numerical purposes \vec{n} can be considered constant.
2. Using the \vec{n} found above, the second order term corrections to \vec{r}_0 and λ_i can be estimated:

$$\begin{aligned} \Delta\lambda_i &= \frac{\lambda_i}{R} (\vec{r}_i - \vec{r}_0) \cdot \vec{n} \times \vec{n}_B \\ \Delta\vec{r}_0 &= \langle \vec{r} \rangle - \vec{r}_0 - \langle \lambda \rangle \vec{n} - \frac{\langle \lambda^2 \rangle}{2R} \vec{n} \times \vec{n}_B \end{aligned} \quad (21)$$

computations again only modestly CPU demanding.

3. Introducing the third order term and using the previously corrected $(\vec{n}, \vec{r}_0, \lambda_i)$, local and global equations for the parameters can be written:

$$\begin{aligned} (\vec{n} + \lambda_i \mathbf{F} \vec{n} + \frac{\lambda_i^2}{2} \mathbf{G} \vec{n}) \cdot \vec{\rho}_i &= 0 \\ \langle (\lambda \cdot \mathbf{1} - \frac{\lambda^2}{2} \mathbf{F} + \frac{\lambda^3}{6} \mathbf{G}) \vec{\rho} \rangle &= 0 \\ \langle \vec{\rho} \rangle &= 0 \end{aligned} \quad (22)$$

where $\vec{\rho}_i$ are the residuals of the points to the fitted curve:

$$\vec{\rho}_i = -\vec{r}_i + \vec{r}_0 + \lambda_i \vec{n} + \frac{\lambda_i^2}{2} \mathbf{F} \vec{n} + \frac{\lambda_i^3}{6} \mathbf{G} \vec{n} \quad (23)$$

Expanding to first order, the corresponding corrections $(\Delta \vec{n}, \Delta \vec{r}_0, \Delta \lambda_i)$ must satisfy:

$$\begin{aligned} \alpha_i \Delta \lambda_i + \vec{a}_i \cdot \Delta \vec{n} + \vec{b}_i \cdot \Delta \vec{r}_0 + \beta_i &= 0 \\ \langle \vec{a} \Delta \lambda \rangle + \langle \lambda^2 \rangle \mathbf{1} \cdot \Delta \vec{n} + \mathbf{D} \Delta \vec{r}_0 + \vec{\delta} &= 0 \\ \langle \vec{b} \Delta \lambda \rangle + \mathbf{D}^\dagger \Delta \vec{n} + \mathbf{1} \cdot \Delta \vec{r}_0 + \vec{\sigma} &= 0 \end{aligned} \quad (24)$$

where:

$$\begin{aligned} \alpha_i &= \vec{n}^2 - \vec{r}_i \cdot \mathbf{F} \vec{n} + \vec{r}_0 \cdot \mathbf{F} \vec{n} \\ \beta_i &= \vec{r}_0 \cdot \vec{n} - \vec{r}_i \cdot \vec{n} + \lambda_i \vec{n}^2 + \lambda_i \vec{r}_0 \cdot \mathbf{F} \vec{n} - \\ &\quad \lambda_i \vec{r}_i \cdot \mathbf{F} \vec{n} + \frac{1}{2} \lambda_i^2 \vec{r}_0 \cdot \mathbf{G} \vec{n} - \frac{1}{2} \lambda_i^2 \vec{r}_i \cdot \mathbf{G} \vec{n} + \\ &\quad \frac{1}{6} \lambda_i^3 \vec{n} \cdot \mathbf{G} \vec{n} \\ \vec{a}_i &= \vec{r}_0 - \vec{r}_i + 2\lambda_i \vec{n} + \lambda_i \mathbf{F} \vec{r}_i - \lambda_i \mathbf{F} \vec{r}_0 \\ \vec{b}_i &= \vec{n} + \lambda_i \mathbf{F} \vec{n} \\ \vec{\delta} &= \langle \lambda \rangle \vec{r}_0 - \langle \lambda \vec{r} \rangle + \langle \lambda^2 \rangle \vec{n} + \frac{1}{2} \mathbf{F} \langle \lambda^2 \vec{r} \rangle - \\ &\quad \frac{1}{2} \langle \lambda^2 \rangle \mathbf{F} \vec{r}_0 + \frac{1}{6} \langle \lambda^3 \rangle \mathbf{G} \vec{r}_0 - \frac{1}{6} \mathbf{G} \langle \lambda^3 \vec{r} \rangle + \\ &\quad \frac{1}{12} \langle \lambda^4 \rangle \mathbf{G} \vec{n} \\ \vec{\sigma} &= \vec{r}_0 - \langle \vec{r} \rangle + \langle \lambda \rangle \vec{n} + \frac{1}{2} \langle \lambda^2 \rangle \mathbf{F} \vec{n} + \frac{1}{6} \langle \lambda^3 \rangle \mathbf{G} \vec{n} \\ \mathbf{D} &= \langle \lambda \rangle \mathbf{1} - \frac{1}{2} \langle \lambda^2 \rangle \mathbf{F} \end{aligned} \quad (25)$$

By eliminating $\Delta \lambda_i = -(\beta_i + \vec{a}_i \Delta \vec{n} + \vec{b}_i \Delta \vec{r}_0) / \alpha_i$ equations (24) become:

$$\begin{aligned} \mathbf{M} \Delta \vec{n} + \mathbf{N} \Delta \vec{r}_0 &= \vec{\tau} \\ \mathbf{N}^\dagger \Delta \vec{n} + \mathbf{R} \Delta \vec{r}_0 &= \vec{\pi} \end{aligned} \quad (26)$$

where:

$$\begin{aligned} \mathbf{M} &= \left\langle \frac{\vec{a} \vec{a}}{\alpha} \right\rangle - \langle \lambda^2 \rangle \mathbf{1} \\ \mathbf{N} &= \left\langle \frac{\vec{a} \vec{b}}{\alpha} \right\rangle - \langle \lambda \rangle \mathbf{1} + \frac{1}{2} \langle \lambda^2 \rangle \mathbf{F} \\ \mathbf{R} &= \left\langle \frac{\vec{b} \vec{b}}{\alpha} \right\rangle - \mathbf{1} \end{aligned} \quad (27)$$

and :

$$\begin{aligned} \vec{\tau} &= \vec{\delta} - \left\langle \frac{\beta \vec{a}}{\alpha} \right\rangle \\ \vec{\pi} &= \vec{\sigma} - \left\langle \frac{\beta \vec{b}}{\alpha} \right\rangle \end{aligned} \quad (28)$$

To zeroth order the three \mathbf{M} , \mathbf{N} and \mathbf{R} tensors are proportional to $(\mathbf{1} - \vec{n} \vec{n})$, the non-invertable perpendicular projection to \vec{n} , by factors of $\langle \lambda^2 \rangle$, $\langle \lambda \rangle$ and 1. Therefore in the numerical approach, the inversion is obtained by decomposing the operators into a part proportional to $(\mathbf{1} - \vec{n} \vec{n})$ and a “remainder”:

$$\mathbf{R} = (\mathbf{1} - \vec{n} \vec{n}) \cdot (2 \text{tr} \mathbf{R} - \mathbf{R}_{\vec{n} \vec{n}} - \mathbf{R}_{\vec{n} \vec{n}}^\dagger) / 4 + \dots \quad (29)$$

The solution $(\Delta \vec{n}, \Delta \vec{r}_0, \Delta \lambda_i)$ is therefore:

$$\begin{aligned} \Delta \vec{n} &= (\mathbf{R} \mathbf{N}^{-1} \mathbf{M} - \mathbf{N}^\dagger)^{-1} (\mathbf{R} \mathbf{N}^{-1} \vec{\tau} - \vec{\pi}) \\ \Delta \vec{r}_0 &= \mathbf{N}^{-1} (\vec{\tau} - \mathbf{M} \Delta \vec{n}) \\ \Delta \lambda_i &= -\frac{1}{\alpha_i} (\beta_i + \vec{a}_i \cdot \vec{n} + \vec{b}_i \cdot \Delta \vec{r}_0) \end{aligned} \quad (30)$$

All quantities in this section were considered normalised - *i.e.* $\sigma^{-1} \vec{r} \rightarrow \vec{r}$, although for notation simplicity they were written as the quantities themselves.

The CPU demand of the above 3 steps is under 15 μs . For better precision however, the last step can be repeated twice, bringing the 3D-helix fit to 22 μs . This is at least 4000 times faster than any iterative version of the fit.

To complete the fit in all generality, dE/dx can be incorporated by perturbatively bending a pure helical track into a dE/dx -helix. This would allow in principle to infer the track’s mass, although with large errors in certain energy ranges.

Using the fit over blocks of 2000 tracks the alignment in magnetic field was checked and adjusted. The fit was then used on blocks of 10 tracks for a fine scan of the beam energy delivered by the SPS to the Test Beam setup. This was expressed in normal-impact radius of curvature equivalent, and it is shown in figure 3 (bottom-right).

VI. ACKNOWLEDGEMENTS

I am thankful to the High Energy Physics group of the Wuppertal University - in particular to Prof. Dr. K.-H. Becks, for the kind hospitality and facilities provided during completion of this work, as well as to the ATLAS Pixel Detector Collaboration for the opportunity of engaging in the Test Beam activity. I would especially like to thank the Alexander von Humboldt Foundation for support during this period and for the opportunity of better knowing German research and culture.

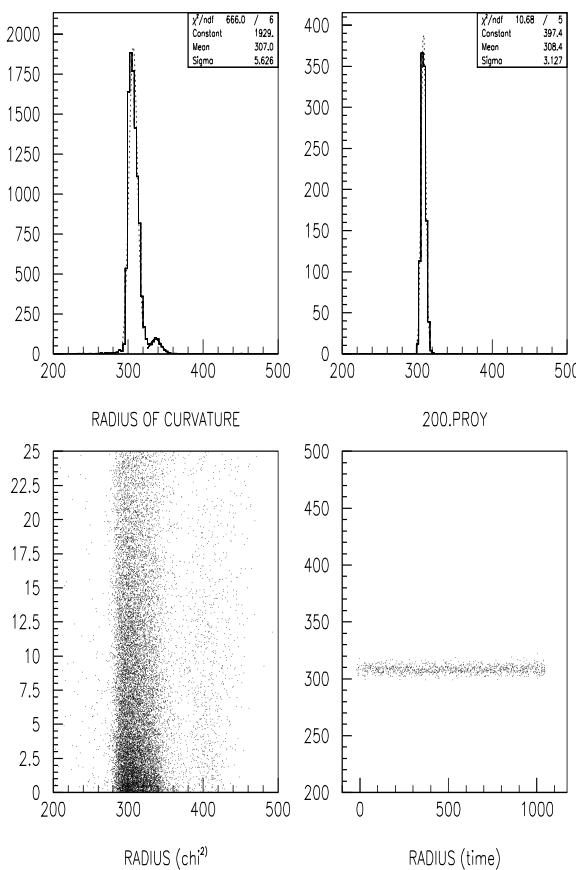


FIG. 3. Normal-impact equivalent radius of curvature for single tracks (top-left) and corresponding χ^2 of fit vs. radius of curvature (bottom-left). The resolution was on the order of 6m and the average radius of curvature 307m. Using blocks of 10 tracks (top-right) the resolution improves to $\simeq 3.3$ m, the stability of the SPS delivered beam being tracked vs. time (bottom-right).

V. CONCLUSIONS

Analytical methods were shown to have a dramatic impact on the speed of line and helix fits, bringing down CPU usage by 3-4 orders of magnitude. The methods developed were successfully tested in the alignment and data reconstruction of the Test Beam results for the ATLAS Pixel Detector MCM-D modules, and can be of great impact for high precision alignment and reconstruction in all pixel detectors. Such routines could be used for instance by the ATLAS Inner Detector to specify precision \vec{p}_\perp corrections to the m_π evaluated mass of B-vertices, in order to strongly suppress c-decay backgrounds.

- [1] M. Dima, SLAC-R-0505, (1997) p. 100.
- [2] P. Avery, KWFIT, CSN98-355, (1998).
- [3] ATLAS Inner Detector TDR, CERN/LHCC/97-16, ISBN 92-9083-102-2; CERN/LHCC/97-17, ISBN 92-9083-103-0.
- [4] I. Ropotori et al., Nucl. Instr. Meth. **A439** (2000), 536.
- [5] F. James, F. Roos, CERN (1967).
- [6] ALEPH Collaboration, CERN-PPE/97-017, (1997).
- [7] SLD Collaboration, SLAC-PUB-7481, (1997).
- [8] Particle Data Group, Euro. Phys. J. **C15** (2000), 1.